Study of Mg Kα x-ray multiplet structure observed in ion-atom collisions

A. Langenberg* and R. L. Watson

Cyclotron Institute and Department of Chemistry, Texas A&M University, College Station, Texas 77843

(Received 11 August 1980)

High-resolution measurements of Mg Kα x-ray spectra excited by 1–3-MeV/amu H^+, He^+, O^{2+}, Ne^{2+}, and S^{4+} ions have been performed for Mg metal and some of its compounds. A detailed examination of the multiplet structure of the KL^1, KL^2, and KL^3 satellite groups revealed substantial variations in the intensities of various components as a function of projectile velocity and atomic number, and as a function of the chemical composition of the target. A theoretical spectrum was constructed using transition energies obtained from "corrected" single-configuration Hartree-Fock results and assuming a statistical population of all initial states belonging to the same electron configuration. This theoretical spectrum agreed quite favorably with the experimental spectrum for Mg metal obtained with 5.4-MeV He^+ ions.

I. INTRODUCTION

$K\alpha$ x-ray satellites result from transitions of the type $1s^{-1}2s^{-i}2p^{-j} \rightarrow 2s^{-i}2p^{-(j+1)}$. A complicated multiplet structure arises as a consequence of the angular-momentum coupling of the multiple inner-shell vacancies and leads to an interspersion of transitions corresponding to different initial-state electron configurations. The interpretation of the complex $K\alpha$ satellite structure observed in ion-excited x-ray spectra in terms of the 90 transitions allowed in LS coupling is a difficult task requiring very accurate theoretical transition energies and probabilities. Additional information obtained by studying the dependence of the structure on projectile atomic number and velocity can be extremely useful in the identification of satellite components which overlap with neighboring satellite groups.

While a considerable amount of work has been done on the identification of the various lines which contribute to the KL^1 satellite group,[1,2] very little has been reported on the multiplet structure of the KL^2, and KL^3 satellite groups. The use of heavy-ion collisions as a means of exciting x-ray emission provides the opportunity of examining these higher-order satellites in considerably more detail than is possible using electron bombardment or photon fluorescence.

In the present work, the $K\alpha$ x-ray spectra of magnesium metal and some of its compounds have been measured using 1–3-MeV/amu H, He, O, Ne, and S ions. From the projectile atomic number and velocity dependencies of these spectra, conclusions were drawn concerning the relative probabilities for $2s$ and $2p$ ionization, and overlapping components from neighboring satellite groups were detected. A detailed analysis of theoretical line energies and intensities, including a systematic study of deviations between experimental and single-configuration Hartree-

Fock energies, enabled the construction of a "theoretical" spectrum. Chemical effects were also examined, and the influence of Coster-Kronig transitions considered. A preliminary report on some of this work was presented in Ref. 3.

II. EXPERIMENTAL

Beams of 1–3-MeV/amu H^+, He^+, O^{2+}, Ne^{2+}, and S^{4+} ions were extracted from the Texas A&M variable energy cyclotron, transmitted through a 30° bending magnet, and focused at the target position by means of a pair of quadrupole magnets. The targets consisted of a 22.1 mg/cm² metallic foil of Mg and thick pressed pellets of MgO, $MgCl_2$, and MgF_2. Mg $K\alpha$ x-ray spectra were measured with a 12.7-cm Johansson-type, curved-crystal spectrometer.[4] The gas-flow proportional counter (90% argon and 10% methane counter gas at 1 atm) had a fixed entrance slit of 0.05-cm width and a 530-μg/cm² mylar window (53% transmission for Mg $K\alpha$ x-rays). This slit width corresponds to a resolution of 1.1 eV at 1253.6 eV (the Mg $K\alpha_{1,2}$ energy) using an ADP (ammonium dihydrogen phosphate) crystal having $2d = 10.642$ Å.

The spectrometer was oriented such that the focal circle was in the horizontal plane and the x rays were observed at an angle of 142.5° with respect to the beam direction. This angle is near the "magic angle" of 125.3° and so polarization effects are not expected to have a measurable influence on the spectra.[5] Variations in crystal reflectivity[6] and x-ray absorption were neglected over the range of transition energies (~10 eV) contained within a single satellite group since it was estimated that they would change the relative line intensities by less than 5%.

Spectra for Mg metal, obtained with 2.75-MeV H^+, 5.4-MeV He^+, and 32-MeV O^{2+} ions, are compared in Fig. 1. The $K\alpha$ satellite groups KL^1, KL^2, KL^3, and KL^4 are readily observable in the
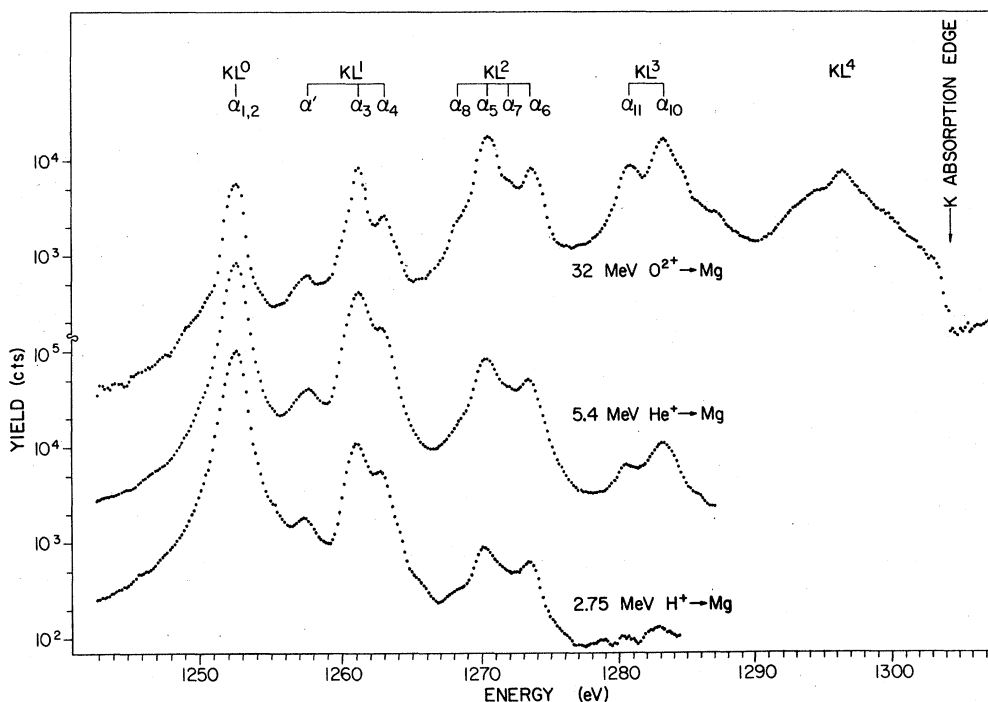
FIG. 1. Mg $K\alpha$ satellite spectra excited by 32-MeV O^{2+}, 5.4-MeV He^+, and 2.75-MeV H^+ ions in thick Mg metal targets. The spectroscopic notation of the satellites $(\alpha_1 \rightarrow \alpha_{11})$ indicates the order of decreasing intensity in the case of electron excitation.

spectrum excited by O ions. The K absorption edge of Mg metal occurs just to the right of the KL^4 satellite group and causes the KL^5 and higher satellites to be greatly attenuated. In the case of MgO, most of the KL^5 satellite group is visible because the absorption edge is 6.9 eV higher than it is in Mg metal. Many of these lines (labeled α_1 to α_{11} in Fig. 1) were observed over 50 years ago in electron- and photon-excitation experiments.[7] The magnification by over three orders of magnitude in the intensity of the KL^3 satellite group, achieved through the use of heavy-ion excitation, clearly reveals more structure than just the α_{11} and α_{10} peaks. The positions of the various peaks do not depend (to within ±0.2 eV) on the atomic number of the exciting ion.

III. INTERPRETATION OF THE MULTIPLET STRUCTURE

A. Dependence on projectile atomic number and velocity

Portions of the $K\alpha$ satellite spectra of Mg metal obtained with a variety of ions are shown in Figs. 2(a), 2(b), and 2(c). For the purposes of comparison, each has been normalized to the highest peak of the satellite group. In Fig. 2(a), it is apparent that the ratio of the α_3 to α_4 intensities increases with increasing projectile atomic number. This

behavior could result from a dependence on projectile Z of (a) the Coster-Kronig transition probability for converting $2s$ holes to $2p$ holes prior to $K\alpha$ x-ray emission, (b) the (nonstatistical) population of initial-state terms, or (c) the relative probability for ionization of $2s$ and $2p$ electrons. It should be noted that α_4 originates from the initial-state vacancy configuration $1s^{-1}2p^{-1}$, whereas α_3 contains contributions from both $1s^{-1}2p^{-2}$ and $1s^{-1}2s^{-1}$ vacancy configurations.

Essentially the same behavior is observed for the KL^2 and KL^3 satellite groups in Fig. 2(b) and (c). The ratios of the intensities of the low-energy components of the satellite groups (α_5 and α_{11}) to those of the high-energy components (α_6 and α_{10}) increase with increasing projectile Z. It would appear, therefore, that the same explanation should apply to all three satellite groups.

With regard to Coster-Kronig transitions, single-configuration Hartree-Fock (SCHF) calculations for free Mg atoms indicate an excess energy of 8.4 eV for KL^1 transitions ($1s^{-1}2s^{-1}$ $\rightarrow 1s^{-1}2p^{-1}3p^{-1}$), but increasingly negative energies for KL^2 and KL^3 transitions (-10.5 and -69.2 eV, respectively). Bhalla and Richard[8] have similarly concluded that Coster-Kronig transitions are not energetically possible from KL^2 and KL^3 initial states of Al, based on the results of Hartree-
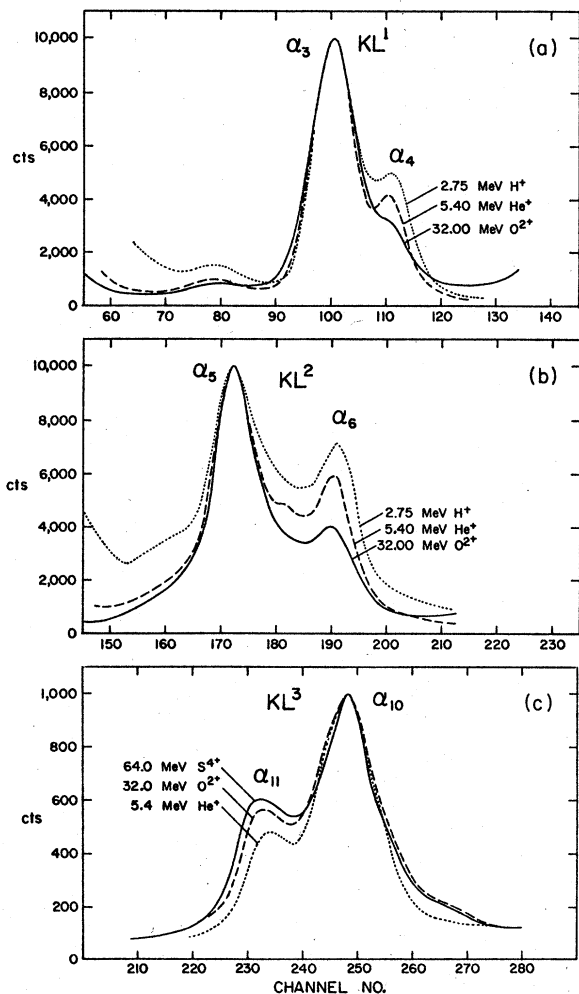
FIG. 2. Portions of $K\alpha$ satellite spectra of Mg observed with a variety of projectiles in thick Mg metal targets, normalized to the highest peak of the satellite group; (a) KL^1, (b) KL^2, and (c) KL^3 satellite group.

Fock-Slater calculations.

A varying (nonstatistical) population of initial-state terms could account for the changing α_3 to α_4 intensity ratio where α_4 has only one initial-state term (^1P) and α_3 only two (^3S and ^3P). In fact, Bhalla et al.[9] have observed a nonstatistical population of the ^1P and and ^3P terms for the $1s^{-1}2p^{-1}$ configuration of Ne ($^3P/^1P \sim 1.5$). However, the $^3P/^1P$ intensity ratio did not vary with projectile Z. In the case of the KL^2 and KL^3 satellite groups, the peaks under consideration are composed of lines from a number of different terms and one would expect preferential population to have a much smaller net effect.

The calculations described in the following section indicate that, in general, screening by $2s$ electrons leads to higher transition energies than screening by $2p$ electrons. The high-energy
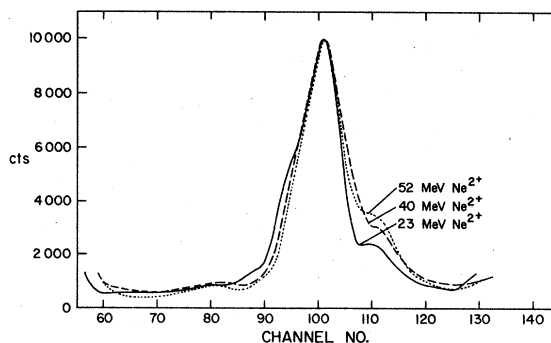

FIG. 3. KL^1 satellite group of Mg observed with Ne^{2+} ions of different velocities.

peaks in each satellite group are, therefore, mainly composed of transitions from initial states having $2p$ rather than $2s$ vacancies. Hence, the varying intensity ratios (α_3/α_4, α_5/α_6, and α_{11}/α_{10}) most likely indicate that the probability for $2s$ ionization increases relative to that for $2p$ ionization as the projectile atomic number increases.

A comparison of the KL^1 satellite groups obtained using Ne ions at several different velocities is shown in Fig. 3. It is apparent that the α_4 to α_3 intensity ratio increases with increasing ion velocity, and approaches the ratio displayed by the light ion (H^+ and He^+) spectra. This observation, in conjuction with the above conclusion, indicates that the probability for $2s$ ionization decreases relative to that for $2p$ ionization as the projectile velocity increases. A quantitative study of the velocity and Z dependences of the $2s$ and $2p$ ionization probabilities for Mg is currently in progress.

Another interesting feature in Fig. 3 is the bump on the low-energy side of α_3, the intensity of which decreases with increasing ion velocity. The multiplet structure calculations (next section) reveal the presence of a KL^2 transition with just the right energy to explain this feature. The fact that the KL^2 satellite group relative intensity decreases with increasing ion velocity is consistent with this interpretation. This observation emphasizes the need for caution in estimating satellite group total intensities and in analyzing x-ray polarization results.

B. Comparison with theoretical calculations

1. Survey of calculational results

The first calculations of $K\alpha$ x-ray satellite transition energies were performed by Kennard and Ramberg[10] using the Hartree-Fock method. Asaad[11] and Gabriel[12] improved these calculations

by including interactions between terms having the same n, L, S, and parity. Coefficients for the off-diagonal elements had been published as early as 1937 (Ref. 13). Detailed transition energy calculations for the $K\alpha$ satellites of Ne have been carried out by Matthews et al.[14] using the single-configuration Hartree-Fock (SCHF) method, and by Bhalla[15] using the Hartree-Fock-Slater (HFS) method. In the calculations of Matthews et al.,[14] however, the nondiagonal matrix components between multiplets having the same total L and S (which arise in cases involving three open sub-shells) were neglected. Multiconfiguration Hartree-Fock (MCHF) calculations including spin-orbit interactions have recently been performed by Fischer and Ridder[16] for the $2p^{-1}3p^{-1}$ initial states of Ar L x-ray satellites. The addition of 47 configurations did not result in a significant improvement in the agreement with the experimental measurements of Nordgren et al.[17]

Z-expansion calculations were first employed by Layzer[18] in 1959. This method simultaneously provides results for all members of an isoelectronic sequence and has the additional advantage that relativistic terms are easily added. Based on this method, Horak[19] obtained semiempirical results for the KL^1 satellites of Ne through Si (without relativistic terms). The third term of the expansion was adjusted to give agreement with optical data (final states) and K x-ray data for Ne (initial states). Other Z-expansion calculations have been performed by Hartmann and Hendal,[20] and by Safronova and co-workers.[21] Tables are now available for various states in

(a) He-like ions with filled K shells (6 terms), (b) some ions with KL^5 and KL^7 vacancy configurations (5 and 6 terms, respectively), and (c) a few ions with KL^4, KL^5, and KL^6 vacancy configurations (3 terms; nonrelativistic). There are, however, no published Z-expansion results for the satellites of primary interest in the present work; namely those associated with KL^1, KL^2, and KL^3 vacancy configurations.

An assessment of the accuracy of the calculational methods discussed above, as applied to several of the energy levels in Ne^{2+} (i.e., Ne III), is provided by Table I. In this table, the electron configuration is specified by the notation $[ijk]$ where i, j, and k, respectively, indicate the numbers of $1s$, $2s$, and $2p$ electrons present. The results of the various calculations are compared with experimental energies obtained from the optical data compilation of Moore.[23] Absolute energies were derived by adding the differences between the term energies to the sum of the ionization limits for Ne X to Ne IV. As is indicated at the bottom of Table I, the average deviation between the experimental and theoretical energies is quite large ($\sim$12 eV) for all but the 6-term Z-expansion calculations. Also, the ratio of the energy difference between S and D terms to that between D and P terms given by SCHF deviates significantly from the experimental value. Since differences in adjacent line energies for the $K\alpha$ x-ray satellite spectrum of Ne are typically about 0.6 eV, it is evident that better accuracy than is provided by SCHF or 3-term Z- expansion calculations will be required for correct identification of the observed structure.

TABLE I. Atomic energy levels for Ne III (in eV).

Electron configuration	Term	SCHF[a]	SCHF + CI[b]	Z-exp[c] (3 terms)	Z-exp[c] (6 terms)	Semiempirical[d]	Experiment[e]
[224]	^1S	−3430.27	−3432.28	−3431.27	−3442.06	−3430.18	−3442.81
	^1D	−3435.39		−3435.15	−3445.65	−3433.89	−3446.22
	^3P	−3438.80		−3438.61	−3448.97	−3437.06	−3449.68
[215]	^1P	−3400.14		−3400.50	−3412.43	−3401.21	−3413.83
	^3P	−3412.36		−3412.06	−3423.09	−3411.73	−3424.36
[206]	^1S	−3376.34	−3374.33	−3376.14	−3389.21	−3377.10	
Average deviation		12.06	11.65	11.92	1.00	12.63	
Standard deviation[f]		1.13	1.26	0.90	0.32	0.00	
Ratio $(S-D)/(D-P)$		1.50	0.91	1.12	1.08	1.17	1.17

[a] Calculated using the Hartree-Fock program of Fischer (Ref. 22).
[b] Same as (a) but with configuration interaction between ^1S terms included.
[c] From Safronova et al. (Ref. 21).
[d] From Horak (Ref. 19).
[e] From the optical data compilation of Moore (Ref. 23).
[f] Standard deviation of the energy differences with respect to the experimental values.

2. Study of deviations from SCHF results for He- to Ne-like ions

Because of the relative ease and convenience with which SCHF calculations can be performed, it is of interest to investigate ways in which the results of such calculations can be corrected to improve the accuracy of predicted transition energies. With this goal in mind, a study of the deviations between experimental and SCHF energies for He- to Ne-like ions was carried out, as suggested by the work of Edlen.[24,25]

The Hartree-Fock program of Fischer[22] was used to calculate the average energy of configuration and the values of the Slater Coulomb (F^k) and exchange (G^k) integrals. The LS-term energies were then determined in the usual manner.[26] Calculations were performed for configurations ($[ijk]$) with $i=2$, $j=0$, 1, 2, and $k=0$ to 6, for elements $Z=8$ to 14. The SCHF energies were compared with accurate experimental energies derived from optical spectra,[23] which had been averaged with weights proportional to $2J+1$.

The results are presented in Figs. 4 through 8 in the form of ratios of experimental to SCHF energy differences. In Fig. 4, ΔE is $E_{av}[2jk]$ $-E_{av}[22k]$ where E_{av} is the average energy of the configuration for Mg. In Fig. 5, similar ratios of energy differences are given relative to the E_{av} of the Ne-like configuration of the same element (i.e., $\Delta E = E_{av}[2jk] - E_{av}[226]$.

The ratio of the energy difference between S and D terms to the energy difference between D and P terms of the same electron configuration is shown as a function of atomic number in Fig. 6. The solid curves show the ratios obtained
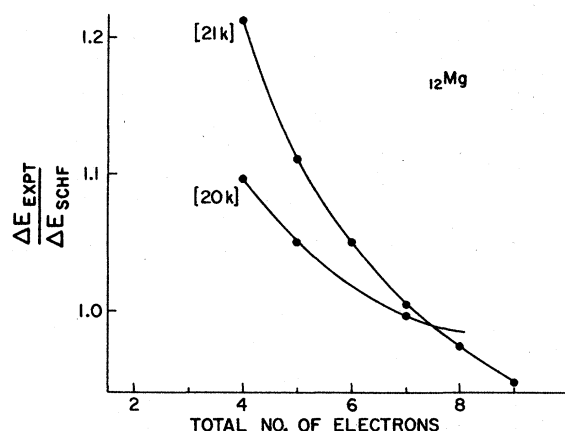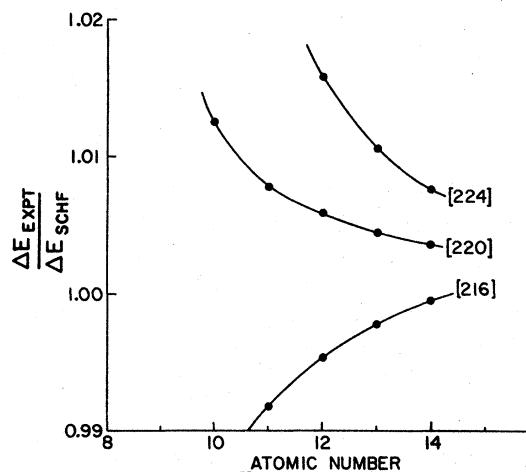

FIG. 5. Ratios of experimental (Ref. 23) to SCHF average of configurations energy differences as a function of atomic number ($\Delta E = E_{av}[2jk] - E_{av}[226]$ where j and k are specified by the configuration label in the figure).

from the optical data, whereas the dashed line shows the ratio predicted by SCHF. The SCHF ratio is independent of the electron configuration and the atomic number, while the optical data ratios display a dependence on both of these quantities.

Ratios of experimental to SCHF energy differences between terms belonging to the same electron configuration are shown as a function of atomic number in Figs. 7 and 8. For the configurations in Fig. 7, the SCHF term energy differences are given by $6/25F^2(2p,2p)$ while

FIG. 4. Ratios of experimental (Ref. 23) to SCHF average of configurations energy differences for Mg as a function of total number of electrons. ($\Delta E = E_{av}[2jk]$ $- E_{av}[22k]$ where j is specified by the configuration label in the figure and $k = n - j - 2$ where $n =$ total number of electrons.)
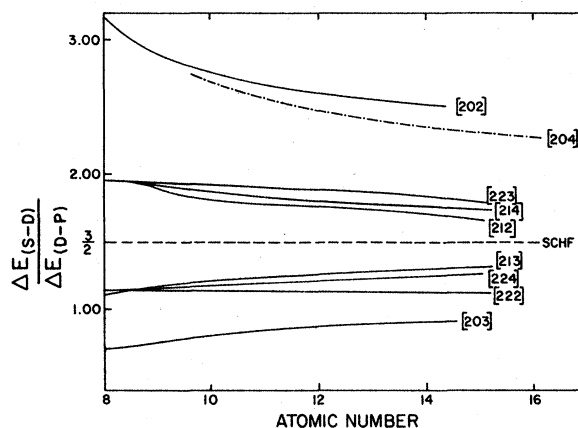
FIG. 6. Ratios of energy differences between S and D terms to energy differences between D and P terms for various electron configurations as a function of atomic number. The solid curves show the ratios obtained from experimental data (Ref. 23) and the dashed curve shows the SCHF prediction for all configurations. The dot-dashed curve indicates the results of 3-term nonrelativistic Z-expansion calculations (Ref. 21) for the [204] configuration, for which experimental data were unavailable.
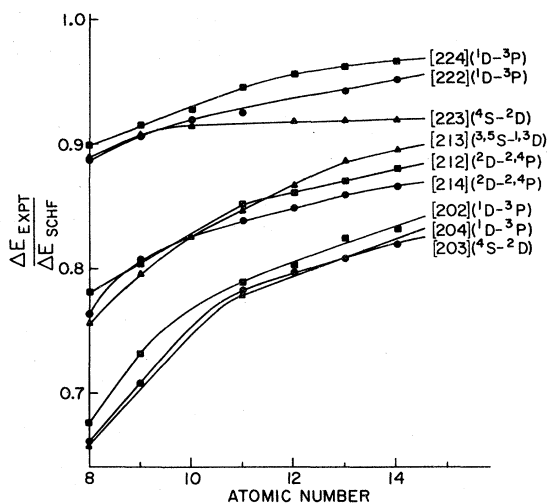
FIG. 7. Ratios of experimental (Ref. 23) to SCHF energy differences between terms belonging to the same electron configuration, as a function of atomic number. ($\Delta E_{\text{SCHF}} = 6/25F^2(2p, 2p).$)

those for the configurations in Fig. 8 are given by $2/3G^1(2s, 2p)$ (Ref. 26). As may be seen from these figures, SCHF calculations overestimate the multiplet splittings by as much as 35%, but this tendency decreases as the atomic number increases. A similar conclusion was reached by Fisher and Ridder[16] who found that by scaling down the F^k and G^k integrals by a factor of 0.88, the ordering of terms and the multiplet splittings could be brought into better agreement with experiment.

3. Semiempirical analysis of the Kα x-ray satellite spectrum of Mg

In order to obtain an accuracy of the order of 0.5 eV for Mg Kα x-ray transition energies (~1250 eV), it is necessary to compute the total energies of the initial and final states with an accuracy of 1 part in 10^4. Since present day *ab initio* methods appear to be incapable of this
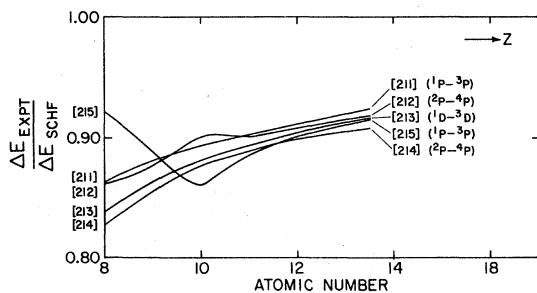

FIG. 8. Ratios of experimental (Ref. 23) to SCHF energy differences between terms belonging to the same electron configuration, as a function of atomic number. ($\Delta E_{\text{SCHF}} = 2/3G^1(2s, 2p).$)

task (see Sec. III B 1), the analysis of the Kα x-ray satellite spectrum of Mg was performed using the "corrected" SCHF results described in the preceding section. The procedure adopted for the calculation of transition energies was as follows: (a) The SCHF final-state energies were corrected using the correction factors given in Figs. 4 to 8 for Mg. (b) The SCHF initial-state energies were corrected using correction factors for the next element Al to approximately account for the effect of the 1s hole (equivalent core approximation). A justifiable way to correct the remaining contributions to the multiplet energies from the 1s hole [i.e., $G^0(1s, 2s)$ and $G^1(1s, 2p)$] could not be found and so the uncorrected SCHF values were used. The Mg Kα x-ray transition energies, calculated as outlined above, are listed in Table II. All of the configurations considered contained a filled 3s subshell, as is indicated by the last digit in the initial electron configuration specification.

The relative intensities listed in Table II were determined by assuming that all the initial states were populated statistically. In this case, a transition intensity is proportional to $(2L + 1)$ $(2s + 1)\omega_{LS}$ where ω_{LS} is the fluorescence yield. Values of ω_{LS} for Mg were obtained by scaling the results of Bhalla's calculations[27] for N, F, and Ne according to the relationship

$$\omega_{LS}/(1 - \omega_{LS}) \propto Z^4,$$

as suggested by the work of Wentzel.[28] Comparison of Bhalla's values for Ne with those for N confirmed that the theoretical predictions followed this Z dependence to within a few percent.

A "theoretical" spectrum was constructed for the KL^1, KL^2, and KL^3 satellites of Mg from the energies and intensities listed in Table II. Each line was represented by a Voigt profile having a Gaussian width determined by the instrumental resolution and a Lorentzian width equal to twice the corresponding natural linewidth calculated for Ne by Chen and Crasemann.[29] The scale factor of 2 was deduced from a least-squares analysis of the $K\alpha_{1,2}$ peak using a Voigt line shape with variable Lorentzian and Gaussian widths. This analysis yielded a natural linewidth of 0.45 eV for the Mg $K\alpha_{1,2}$ transitions. The theoretical spectrum is compared with an experimental spectrum obtained with 5.4-MeV He⁺ ions in Fig. 9. The resolution of the experimental spectrum has been improved by about 30% by means of an iterative deconvolution procedure (method of ordinate ratio corrections[30]). In Fig. 9, it is apparent that the predicted structural features are in fairly good agreement with the experimental spectrum, but that the predicted relative inten-

TABLE II. Calculated Mg Kα x-ray transition energies and relative intensities.

Satellite group	Initial electron configuration	Transition	E_λ(eV)	I_{rel}	Satellite group	Initial electron configuration	Transition	E_λ(eV)	I_{rel}
KL^0	1262	$^2S \to {}^2P$	1252.8	1.000			$^2S \to {}^2P$	1298.4	0.058
KL^1	1162	$^1S \to {}^1P$	1257.1	0.120			$^4P \to {}^4S$	1293.0	0.225
		$^3S \to {}^3P$	1261.4	0.553		1132	$^2D_- \to {}^2P$	1284.5	0.018
	1252	$^1P \to {}^1S$	1258.2	0.120			$\to {}^2D$	1295.5	0.373
		$\to {}^1D$	1263.3	0.581			$^2D_+ \to {}^2P$	1291.7	0.110
		$^3P \to {}^3P$	1261.6	1.000			$\to {}^2D$	1302.8	0.063
KL^2	1062	$^2S \to {}^2P$	1269.1	0.181			$^2P_- \to {}^2S$	1293.2	0.121
	1152	$^2P_- \to {}^2S$	1263.5	0.066			$\to {}^2P$	1290.2	0.013
		$\to {}^2P$	1260.7	0.153			$\to {}^2D$	1301.3	0.155
		$\to {}^2D$	1270.9	0.752			$^2P_+ \to {}^2S$	1300.5	0.015
		$^2P_+ \to {}^2S$	1270.3	0.013			$\to {}^2P$	1297.5	0.079
		$\to {}^2P$	1267.4	0.263			$\to {}^2D$	1308.6	0.019
		$\to {}^2D$	1277.7	0.068			$^2S \to {}^2P$	1298.2	0.332
		$^4P \to {}^4P$	1270.3	1.000			$^4D \to {}^4P$	1294.2	0.395
	1242	$^2D \to {}^2P$	1268.8	0.164			$^4P \to {}^4P$	1300.0	0.316
		$\to {}^2D$	1272.4	0.481			$^4S_- \to {}^4P$	1295.7	1.000
		$^2P \to {}^2P$	1270.5	0.400			$^4S_+ \to {}^4P$	1312.0	0.010
		$\to {}^2D$	1274.0	0.658			$^4S \to {}^4P$	1275.2	0.151
		$^2S \to {}^2P$	1272.7	0.146		1222	$^2D \to {}^2P$	1297.9	0.143
		$^4P \to {}^4S$	1270.8	0.458			$^2P \to {}^2P$	1300.3	0.583
KL^3	1052	$^1P \to {}^1S$	1273.6	0.062			$^2S \to {}^2P$	1304.0	0.039
		$\to {}^1D$	1283.4	0.315			$^4P \to {}^2P$	1288.7	0.125
		$^3P \to {}^3P$	1280.7	0.594	KL^5	1032	$^1D \to {}^1D$	1309.5	0.086
	1142	$^1D \to {}^1P$	1274.0	0.064			$^1P \to {}^1S$	1305.8	0.031
		$\to {}^1D$	1279.2	0.171			$\to {}^1D$	1317.4	0.039
		$^1P \to {}^1P$	1280.9	0.211			$^3D \to {}^3P$	1306.1	0.094
		$\to {}^1D$	1286.1	0.352			$^3P \to {}^3P$	1314.0	0.076
		$^1S \to {}^1P$	1282.2	0.052			$^3S \to {}^3P$	1310.9	0.432
		$^3D \to {}^3P$	1278.6	0.285			$^5S \to {}^3P$	1295.1	0.040
		$\to {}^3D$	1283.7	0.843		1122	$^1D \to {}^1P$	1307.1	0.024
		$^3P_- \to {}^3S$	1267.9	0.022			$^1P \to {}^1P$	1314.4	0.146
		$\to {}^3P$	1278.8	0.597			$^1S \to {}^1P$	1313.4	0.007
		$\to {}^3D$	1283.9	1.000			$^3D \to {}^3P$	1311.1	0.122
		$^3P_+ \to {}^3S$	1279.8	0.262			$^3P_- \to {}^3P$	1312.1	0.737
		$\to {}^3P$	1290.7	0.025			$^3P_+ \to {}^3P$	1323.6	0.013
		$\to {}^3D$	1295.8	0.037			$^3S \to {}^3P$	1317.5	0.057
		$^3S \to {}^3P$	1286.8	0.279			$^5P \to {}^3P$	1294.0	1.000
		$^5P \to {}^5S$	1282.2	0.903		1212	$^1P \to {}^1S$	1316.3	0.081
	1232	$^1D \to {}^1D$	1285.1	0.593	KL^6	1022	$^2D \to {}^2P$	1323.8	0.106
		$^1P \to {}^1S$	1283.8	0.187			$^2P \to {}^2P$	1327.3	1.000
		$\to {}^1D$	1289.1	0.233			$^2S \to {}^2P$	1336.5	0.048
		$^3D \to {}^3P$	1282.8	0.536			$^4P \to {}^2P$	1314.5	0.086
		$^3P \to {}^3P$	1286.8	0.375		1112	$^2P_- \to {}^2S$	1326.6	0.710
		$^3S \to {}^3P$	1286.1	0.609			$^2P_+ \to {}^2S$	1338.0	0.018
KL^4	1042	$^2D \to {}^2P$	1287.6	0.057			$^4P \to {}^2S$	1313.6	0.696
		$\to {}^2D$	1294.8	0.175	KL^7	1012	$^1P \to {}^1S$	1344.9	1.000
		$^2P \to {}^2P$	1290.4	0.147			$^3P_1 \to {}^1S$	1335.8	1.000
		$\to {}^2D$	1297.6	0.251					

sities for the lines contributing to the KL^2 and KL^3 satellite groups do not provide a very good representation of the observed structure. Part of the problem with the relative intensities is attributable to the fact that the $2s$ and $2p$ ionization probabilities are functions of projectile velocity and atomic number, as discussed in Sec. III A.

Thus the assumption that all initial states are populated statistically is not very satisfactory.

In an effort to ascertain how well the experimental spectrum could be represented by allowing the relative $2s$ and $2p$ ionization probabilities to vary, a least-squares peak fitting analysis was performed. In this analysis, each line was

FIG. 9. Comparison of a measured and calculated K x-ray satellite spectrum for (thick) Mg metal excited by 5.4-MeV He⁺ ions.

represented by a Voigt profile having a variable Gaussian width determined by the experimental resolution and a fixed Lorentzian width equal to the estimated natural linewidth, as described above. The line energy separations were fixed at the calculated values listed in Table II and the relative intensities of all lines belonging to the *same* initial-state electron configuration were also held fixed at the calculated values (Table II). In the least-squares fitting procedure, the only variables were the total intensities and positions of the groups of lines belonging to different initial-state electron configurations. For example, in the KL^1 satellite group, only the sum of the intensities and the average energy of all transitions

arising from the electron configuration [116] and the sum of the intensities and the average energy of all transitions arising from the electron configuration [125] were allowed to vary.

The results are shown in Fig. 10 for the KL^1 and KL^2 satellite groups of the spectrum obtained with 5.4-MeV He⁺ ions. The fitted spectrum reproduces the experimental spectrum reasonably well indicating that most of the energy separations and relative intensities are nearly correct. It is readily seen in this figure that transitions arising from initial states having $2p$ vacancies mainly contribute to the high-energy components of the satellite groups while those arising from initial states having $2s$ vacancies

FIG. 10. Least-squares fit of Mg $K\alpha$ x-ray satellite spectrum of Mg metal excited by 5.4-MeV He⁺ ions. In this fit all transitions belonging to the same initial-state electron configuration have fixed peak separations and intensity ratios (calculated values of Table II). Only the Gaussian (instrumental) peak widths and the total intensities and positions of the 5 transition *groups* indicated by solid and dashed lines were adjusted in the least-squares fitting procedure. The small dots show the calculated points while the large dots show the data points.

mainly contribute to the low-energy components. Also the overlap of the two KL^2 lines $[115]^2P_-$ with the KL^1 satellite group is clearly illustrated.

C. Effect of chemical environment

The influence of the chemical enviroment on the $K\alpha$ satellite structure of Mg is examined in Figs. 11, 12, and 13. Some rather striking differences are observed in the (deconvoluted) spectra obtained with Mg metal and the compounds MgO, $MgCl_2$, and MgF_2. One feature of particular interest is the ratio of the intensity of the $K\alpha_4$ peak to the intensity of the $K\alpha_3$ peak (see Fig. 1 for the identification of these peaks). As has been noted several times in the past,[30,31] this intensity ratio increases dramatically in going from Mg metal to MgO [see Figs. 11(a) and 11(b)]. Additional observations, resulting from the present work, are that (a) when light ions (H^+ and He^+) are used to excite $K\alpha$ x-ray emission, the $K\alpha_4/K\alpha_3$ intensity ratios for MgO, $MgCl_2$, and MgF_2 are all much greater than for Mg metal (0.95 ± 0.05 and 0.71 ± 0.09 for the compounds, and 0.56 ± 0.06 and 0.41 ± 0.03 for the metal respectively), and (b) when heavy ions are used to excite $K\alpha$ x-ray emission, the $K\alpha_4/K\alpha_3$ intensity ratios decrease to 0.37 ± 0.04 for the compounds and to 0.27 ± 0.03 for the metal.

According to the calculated transition energies listed in Table II, the $K\alpha_4$ peak is composed almost entirely of the $[125]^1P$ transition, whereas the $K\alpha_3$ peak contains both the $[125]^3P$ transition and the $[116]^3S$ transition (see Fig. 10). It should be noted that these assignments differ from those given by Demekhin and Sachenko,[32] who have also analyzed this intensity effect. The present identification is supported by the Z-expansion calculations of Horak.[19]

Comparison of the spectra in Figs. 11(a) and 11(b) shows that the increase in the intensity of $K\alpha_4$ in going from Mg metal to MgO is accompanied by a decrease in the intensity of $K\alpha_3$. This suggests that the $[116]^3S$ initial states are highly converted to $[125]$ initial states prior to x-ray emission by Coster-Kronig transitions in MgO but not in Mg metal. If all initial states were populated statistically and Coster-Kronig transitions did not occur, the predicted $K\alpha_4/K\alpha_3$ intensity ratio would be 0.37. On the other hand, in the extreme case that all $[116]^3S$ initial states are converted to $[125]^1P$ initial states, the expected intensity ratio would be 1.04. The observed intensity ratios are consistent with these predictions.

Coster-Kronig transitions are known to be extremely sensitive to the transition energy, especially near threshold. Moreover, Citrin[33] has discussed the possibility of interatomic Coster-
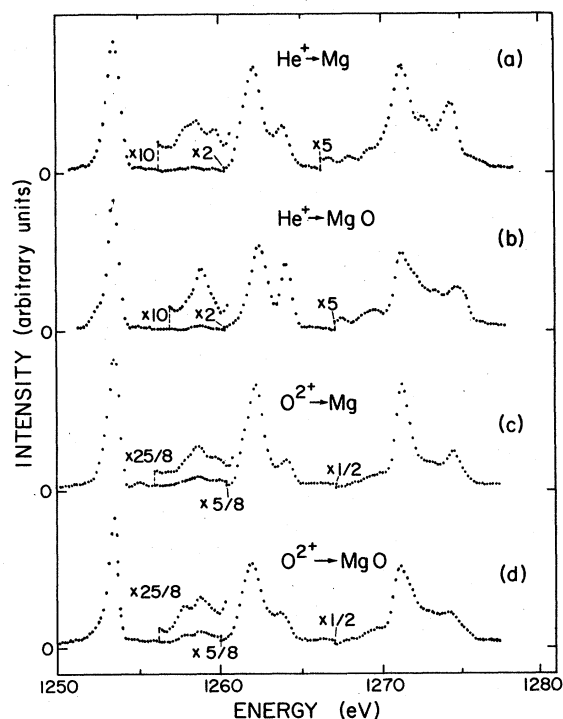

FIG. 11. Mg $K\alpha$ satellite spectra from thick Mg metal targets [(a) and (c)] and thick MgO (b) and (d), excited by 5.4-MeV He^+ [(a) and (b)] and 32-MeV O^{2+} ions (c) and (d).
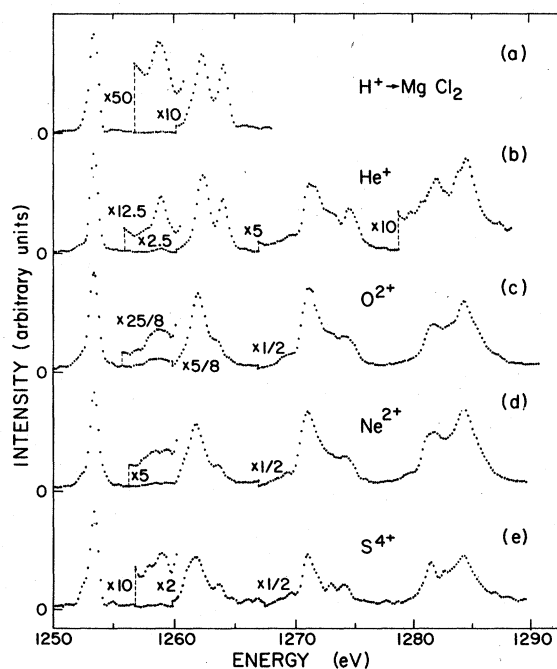

FIG. 12. Mg $K\alpha$ satellite spectra from thick $MgCl_2$ targets excited by (a) 2.75-MeV H^+, (b) 5.4-MeV He^+, (c) 32-MeV O^{2+}, (d) 40-MeV Ne^{2+}, and (e) 64-MeV S^{4+} ions.

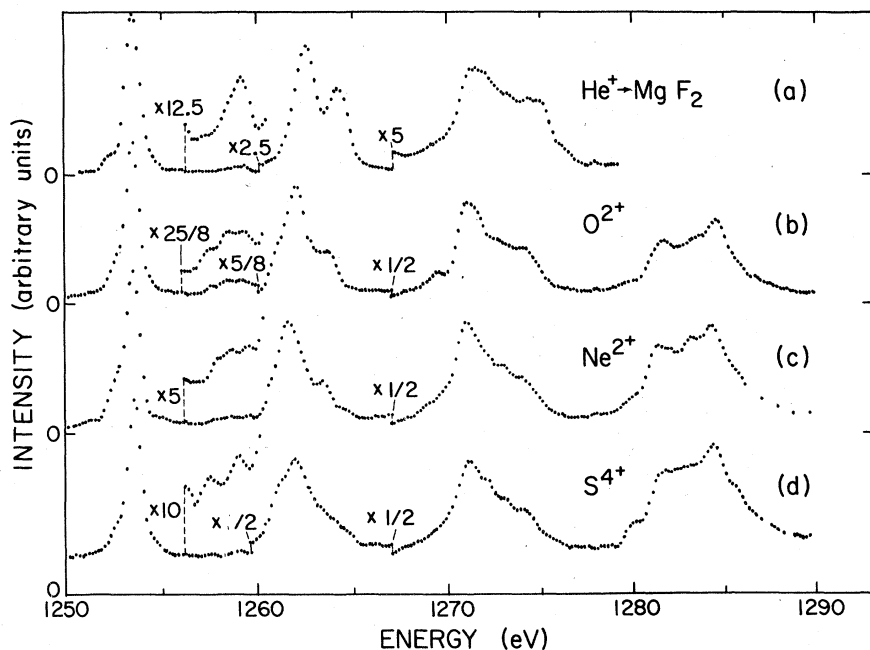FIG. 13. Mg $K\alpha$ satellite spectra from thick MgF_2 targets excited by (a) 5.4-MeV He^+, (b) 32-MeV 0^{2+}, (c) 40-MeV Ne^{2+}, and (d) 64-MeV S^{4+} ions.

Kronig transitions in singly ionized MgF_2 where a $2p$ electron from fluorine fills a $2s$ vacancy in Mg. Such transitions may in fact play a very important role in the deexcitation of the doubly ionized states under consideration here.

In the case of excitation by heavy ions, such as O^{2+}, the $K\alpha_4/K\alpha_3$ intensity ratio does not appear to be as sensitive to the chemical enviroment as when light ions are used. Of course, one must take into account the overlap of the $KL^2[115]^2P$ lines with $K\alpha_3$, since the KL^2 satellites are more intense than the KL^1 satellites in these spectra. Nevertheless, the conclusion is that for heavy-ion excitation, Coster-Kronig transitions contribute less to the observed alterations in the $K\alpha_4/K\alpha_3$ intensity ratios of the Mg compounds than for light-ion excitation. This is probably a result of the higher states of M-shell ionization produced by heavy ions.

Substantial intensity variations and energy shifts are also observed in the $K\alpha_5$ and $K\alpha_6$ peaks of KL^2, and in the $K\alpha_{11}$ and $K\alpha_{10}$ peaks of KL^3 in going from Mg metal to the Mg compounds, as may be seen by comparing Figs. 1, 11, 12, and 13. Because of the complexity of these peaks, not much can be said regarding the causes of the observed variations. Contrary to the case of the KL^1 satellites, however, Coster-Kronig transitions (as was mentioned in Sec. III A) are not expected

to be energetically allowed from KL^2 or KL^3 initial states.

IV. CONCLUSIONS

The multiplet structure of the KL^1, KL^2, and KL^3 x-ray satellite groups of Mg and some of its compounds, excited by ion-atom collisions, has been examined. The relative probabilities for $2s$ and $2p$ ionization were observed to vary with projectile velocity and atomic number. Detailed comparisons of SCHF inital-state energies with those derived from optical data were made and a method for obtaining accurate multiplet transition energies from "corrected" SCHF results was devised. Good agreement between the measured and calculated structure was achieved by assuming a statistical population of all initial states belonging to the same electron configuration, but allowing the relative populations of $2s$ and $2p$ vacancy configurations to be variable. Comparison of spectra for Mg metal, MgO, $MgCl_2$, and MgF_2 revealed sizable peak energy and intensity variations. The role of Coster-Kronig transitions in determining the relative intensities of the KL^1 satellites was considered and found to offer a plausible explanation of the observed difference between the $K\alpha_4/K\alpha_3$ intensity ratio for Mg metal and that for the compounds when excited by light ions.

ACKNOWLEDGMENTS

*Present address: Karolingersweg 146, Wijkbӱ Duurstede, Netherlands 3962 AM.

[1] See L. G. Parratt, Phys. Rev. 50, 1 (1936) and references therein.

[2] See, W. L. Baum and D. W. Fischer, *Spectroscopy of Inorganic Chemistry* (Academic, New York, 1970), Vol. 1, p. 209, and references therein.

[3] R. L. Watson, A. Langenberg, F. E. Jenson, and R. M. Hedges, Jpn. J. Appl. Phys. 17-2, 93 (1978).

[4] Manufactured by Applied Research Laboratories, P.O. Box 129, Sunland, California group, Catalog No. 132 675.

[5] K. A. Jamison and P. Richard, Phys. Rev. Lett. 38, 484 (1977).

[6] D. L. McKenzie, P. B. Landecker, and J. H. Underwood, Space Sci. Instrum. 2, 125 (1976).

[7] E. Hjalmar, Z. Phys. 1-2, 439 (1920); T. Wetterblad, *ibid.* 42, 611 (1927); H. Karlsson and M. Siegbahn, *ibid.* 88, 76 (1934).

[8] C. P. Bhalla and P. Richard, Phys. Lett. 45A, 53 (1973).

[9] C. P. Bhalla, D. L. Matthews, and C. F. Moore, Phys. Lett. 46A, 336 (1974).

[10] E. H. Kennard and E. Ramberg, Phys. Rev. 46, 1040 (1934).

[11] W. N. Asaad, Nucl. Phys. 66, 494 (1965).

[12] A. H. Gabriel, Mon. Not. R. Astron. Soc. 160, 99 (1972).

[13] Hartree and B. Swirles, Proc. Cambridge Philos. Soc. 33, 240 (1937).

[14] D. L. Matthews, B. M. Johnson, and C. F. Moore, At. Data and Nucl. Data Tables 15, 41 (1975).

[15] C. P. Bhalla, Phys. Rev. A 12, 122 (1975).

[16] C. Froese Fischer and D. Ridder, J. Phys. B 11, 2267 (1978).

[17] J. Nordgren, H. Agren, C. Nordling, and K. Siegbahn, in *Proceedings of the International Congress on Physics of x-Ray Spectra, Gaithersburg, Maryland, 1976*, edited by R. D. Deslattes (U.S. G.P.O., Washington, D.C., 1976).

[18] D. Layzer, Ann. Phys. (N.Y.) 8, 271 (1959).

[19] Z. Horak, Proc. R. Soc. London 77, 980 (1961).

[20] H. Hartmann and D. Hendel, Theor. Chim. Acta 15, 303 (1969).

[21] U. I. Safronova and V. N. Kharitonova, Opt. Spektrosk. 27, 300 (1969) [Opt. Spectrosc. (USSR) 4, 550 (1968)]; L. A. Vainshtein and U. I. Safronova, Astron. Zh. 48, 223 (1971) [Sov. Astron. - AJ 15, 175 (1971)]; U. I. Safronova, J. Quant. Spectrosc. Radiat. Transfer 15, 231 (1975).

[22] C. Froese Fischer, Comput. Phys. Commun. 1, 151 (1969).

[23] C. E. Moore, *Atomic Energy Levels*, NBSC No. 467 (Natl. Bur. Stand., Washington, D.C., 1949), Vol. I.

[24] B. Edlen, Phys. Scr. 19, 255 (1979).

[25] B. Edlen, Phys. Scr. 20, 129 (1979).

[26] J. C. Slater, *Quantum Theory of Atomic Structure*, (McGraw-Hill, New York, 1960), Vol. II.

[27] C. P. Bhalla, Phys. Rev. A 12, 122 (1975); C. P. Bhalla, J. Phys. B 8, 2787 (1975).

[28] G. Wentzel, Z. Phys. 43, 524 (1927).

[29] M. H. Chen and B. Crasemann, Phys. Rev. A 12, 959 (1975).

[30] B. Nordfors, Proc. Phys. Soc. A68, 654 (1955); Ark. Fys. 10, 279 (1956).

[31] D. W. Fischer and W. L. Baun, J. Appl. Phys. 36, 534 (1965).

[32] V. F. Demekhin and V. P. Sachenko, Izv. Akad. Nauk SSSR, Ser. Fiz. 31, 912 (1967) [Bull. Acad. Sci. USSR Phys. Ser. 31, 921 (1967)].

[33] P. H. Citrin, J. Electron Spectrosc. Relat. Phenom. 5, 273 (1974).